DE GRUYTER OPEN

Acta Geophysica
vol. 63, no. 1, Feb. 2015, pp. 301-318
DOI: 10.2478/s11600-014-0251-4

Mitigation of Oceanic Tidal Aliasing Errors in Space and Time Simultaneously Using Different Repeat Sub-Satellite Tracks from Pendulum-Type Gravimetric Mission Candidate

Basem ELSAKA[1,2], Karl Heinz ILK[3], and Abdulaziz ALOTHMAN[1]

[1]Space and Aviation Research Institute, King Abdulaziz City for Science and Technology (KACST), Riyadh, Saudi Arabia
e-mail: balsaka@kacst.edu.sa (corresponding author)

[2]National Research Institute of Astronomy and Geophysics (NRIAG), Helwan, Cairo, Egypt

[3]Institute of Geodesy and Geoinformation, University of Bonn, Bonn, Germany

A b s t r a c t

This contribution investigates two different ways for mitigating the aliasing errors in ocean tides. This is done, on the one hand, by sampling the satellite observations in another direction using the pendulum satellite mission configuration. On the other hand, a mitigation of the temporal aliasing errors in the ocean tides can be achieved by using a suitable repeat period of the sub-satellite tracks.

The findings show, firstly, that it is very beneficial for minimizing the aliasing errors in ocean tides to use pendulum configuration; secondly, optimizing the orbital parameter to get shorter repeat orbit mode can be effective in minimizing the aliasing errors. This paper recommends the pendulum as a candidate for future gravity mission to be launched in longer repeating orbit mode with shorter "sub-cycle" repeat periods to improve the temporal resolution of the satellite mission.

Key words: gravity field recovery, repeat sub-satellite tracks, ocean tides aliasing.

1. INTRODUCTION

The products that the twin-satellite GRACE (Gravity Recovery and Climate Experiment) mission (Tapley *et al.* 2004) has provided in the form of numerous model series such as the EIGEN and ITG-GRACE series (*e.g.*, Förste *et al.* 2008, Mayer-Gürr *et al.* 2010), respectively have not yet matched pre-mission expectations in terms of error level and error isotropy. The main limitation of the quality of the resolved temporal gravity field estimates is mostly controlled not only by the instrument noise, but also the anisotropy of spatial sampling and temporal aliasing errors (*i.e.*, the errors in the modeling of mass changes due to the high frequency signals such as atmosphere, ocean, and ocean tides). The latter effects are related to the GRACE orbital configuration because of the inhomogeneous sampling in time and space. Therefore, to minimize the errors in the temporal gravity field models, *e.g.*, ocean tides, one has to optimize and/or improve the determination of the gravitational signal spatially and temporally. On the one hand, a spatially homogeneous sampling can be achieved via the selection of an alternative mission type whose satellite observables are sensitive in other directions (*e.g.*, radial and/or cross-track) compared to the GRACE along-track observable. On the other hand, adjusting the orbit and formation parameters can improve the temporal sampling of the mission. These parameters include the orbital altitude, the inter-satellite distance, the inclination, the repeat mode of sub-satellite tracks (as projected satellite orbits on the Earth's surface) and, of course, the choice of the number of satellites and satellite links to create a possible multi-satellite/formation mission. By means of an appropriate choice of these parameters, isotropy can be enlarged and aliasing effects (the most problematic issue of GRACE mission) can be reduced.

It should be mentioned here that there are common approaches for reducing the temporal aliasing effects, such as smoothing techniques with Gaussian and/or de-correlation filters (see *e.g.*, Wahr *et al.* 2004, Swenson and Wahr 2006, Kusche 2007). However, it was found that the impact of such filters is partially undesirable as a part of the desired gravity signal is smoothed besides the errors.

It is important first to mention that a variety of studies was published in the previous years which have investigated the performance of the basic types of satellite formation missions, *e.g.*, pendulum, cartwheel and LISA (see, *e.g.*, Sharifi *et al.* 2007, Sneeuw *et al.* 2008, Wiese *et al.* 2009, Elsaka *et al.* 2012, 2014a). All these studies have found that the latter three missions would provide a lower error spectrum with improved isotropy. In addition, the arrangement of a second, inclined satellite pair in the so-called "Bender design" was studied by Bender *et al.* (2008), Visser *et al.* (2010), Wiese *et al.* (2011a, 2012), and Elsaka *et al.* (2014b). All of the above-mentioned

studies show a common result that a significant increase in accuracy and sensitivity is expected when a future formation will be flown in an alternative configuration, different from the GRACE leader-follower scheme. Furthermore, Visser *et al.* (2010), Wiese *et al.* (2011b), and Elsaka (2014) have studied the feasibility of estimating low resolution gravity fields at short periods via a single and double pairs of satellites similar to GRACE to reduce the effect of temporal aliasing errors from mass variations with large spatial scales.

The aim of this paper is to focus on reducing the aliasing errors in the ocean tide models in space and time simultaneously, *i.e.*, spatially via selecting the "cross-track" pendulum configuration as an alternative mission candidate for future satellite gravimetry (Elsaka *et al.* 2012, 2014a), and temporally via choosing an appropriate repeat mode of the sub-satellite tracks.

Based on the above-mentioned studies, this paper simulates satellite observations of the "cross-track" pendulum mission, in addition to the GRACE configuration as a reference mission (for a comparative reason), since the other radial configurations are more technically challenging. It is well known that when the GRACE data are analyzed, a set of background models for tidal and non-tidal oceanic, atmospheric and hydrologic mass change are applied to mitigate the aliasing effects; however, remaining errors in these models still alias into the monthly GRACE solutions and manifest themselves as artefacts.

Therefore, this paper applies two oceanic tidal models: FES2004 (Lyard *et al*. 2006) and EOT2008a (Savcenko and Bosch 2008), assuming that the differences of two state-of-the-art oceanic tidal models are representative of their errors. The simulation scenario has been performed using the IGG's GROOPS (Gravity Recovery Object Oriented Programming System) software (Mayer-Gürr 2006), and the gravity results are analyzed in the spectral and spatial domain complete up to degree and order (d/o) 60/60.

This paper is organized as follows: in Section 2, a review concerning the computation of the repeat periods of sub-satellite tracks and the applied repeat modes in this contribution is outlined. The pendulum mission configuration is discussed in Section 3. The simulation strategy used for the gravity field analysis is introduced in Section 4. The gravity field solutions in terms of ocean tide aliasing errors are presented in Section 5. Finally, on this basis, a relevant conclusion is outlined in Section 6.

2. COMPUTATION OF THE REPEAT PERIOD OF SUB-SATELLITE TRACKS

Repeat sub-satellite track means simply that the sub-satellite track retraces itself exactly after a certain time. If the satellite orbit should repeat itself

whilst the Earth was not rotating or the satellite orbital plane was fixed in the Earth's fixed frame, the two satellite crossings at the equator would occur at the same site. Since neither Earth rotation nor the precession of the orbital plane can be neglected, the shift between two ascending nodes takes place. Because the precession of the ascending nodes is much slower than the Earth's rotation, a nodal day differs slightly from a solar day, and in case of a sun-synchronous orbit (*e.g.*, $i = 95°$) they are equal (see Bezděk *et al.* 2009). The nodal day corresponds to the time that the Earth takes to complete one revolution with respect to the orbital plane, while the solar day corresponds to the time required for the Earth to complete one revolution with respect to the Sun–Earth line.

Taking the Earth's rotation rate ($\dot{\omega}$) with respect to the satellite's orbital plane, the notion of a nodal period (P_n) is therefore orbit-dependent and is defined as (after Rees 2001)

$$P_n = \frac{2\pi}{\dot{\omega}} = \frac{2\pi}{(\omega - \dot{\Omega})}\,, \tag{1}$$

where ω is the angular velocity of the Earth, and $\dot{\Omega}$ is the precession rate of the satellite's line of node. After an integer number (α) of Earth rotations in the time required for the satellite to make an integral number of orbits (β), the condition in Eq. 1 can be written as

$$P_n(\omega - \dot{\Omega}) = 2\pi\frac{\alpha}{\beta}\,. \tag{2}$$

The nodal period is equal to the Keplerian period if the perturbations were absent. However, in presence of perturbations, the secular change in the satellite's argument of perigee $\dot{\omega}$ and the secular change in the satellite's mean anomaly $\dot{M}$ must be taken into account (*i.e.*, $P_n = 2\pi/(\dot{\omega} + \dot{M})$). Thus, Eq. 2 can be rewritten in terms of the classical orbital elements as

$$P_n = 2\pi\frac{\alpha}{\beta(\omega - \dot{\Omega})} = \frac{2\pi}{(\dot{\omega} + \dot{M})}\,, \tag{3}$$

and hence,

$$\alpha(\dot{\omega} + \dot{M}) \approx \beta(\omega - \dot{\Omega})\,. \tag{4}$$

Equation 4 represents the repeat period condition and establishes the synchronicity between the Earth rotation and the satellite rotation in a way that the satellite completes β nodal revolutions while the Earth performs α rotations. The three secular changes, $\dot{\omega}$, $\dot{M}$, and $\dot{\Omega}$, in Eq. 2 are calculated according to Kaula (1966) as

$$\begin{aligned}
\frac{\mathrm{d}\Omega}{\mathrm{dt}} &= \frac{3nC_{20}R^2}{2a^2(1-e^2)^2}\cos i\ , \\
\frac{\mathrm{d}\omega}{\mathrm{dt}} &= \frac{3nC_{20}R^2}{4a^2(1-e^2)^2}(1-5\cos^2 i)\ , \\
\frac{\mathrm{d}M}{\mathrm{dt}} &= n-\frac{3nC_{20}R^2}{2a^2(1-e^2)^{3/2}}(3\cos^2 i-1)\ ,
\end{aligned} \tag{5}$$

where n is the satellite's mean motion, C_{20} is the second zonal term of the geopotential, R is the Earth's radius, a is the orbital semi-major axis, and e is the orbital eccentricity. When the Earth takes approximately 365.25 days to orbit around the Sun, this means that it performs exactly 1.002737925 rev (*i.e.*, 1 + 1/365.25) per day. In this way, the duration of the sidereal day becomes exactly 23.9345 hours and the Earth's angular velocity reads $\omega = 2\pi/23.6345 \times 60 \times 60 = 7.2921 \times 10^{-5}$ rad/s.

The repeat period condition (Eq. 3) is related to the mean motion of the satellite, after neglecting the term e^2 (due to its small value) in Eq. 5, using the nodal period of the satellite $2\pi/(\dot{\omega}+\dot{M})$, and the nodal day $2\pi/(\omega-\dot{\Omega})$, as

$$n = \frac{\alpha}{\beta}(\omega-\dot{\Omega})-(\dot{\omega}+\dot{M})\ . \tag{6}$$

After one inserts the secular rates calculated from Eq. 5 into Eq. 4, the ratio β/α can be easily computed. Equation 6 reads for the first order in J_2 (where J_2 is the normalized coefficient $C_{20}\sqrt{5}$) according to Bezděk *et al.* (2009) as

$$n = \frac{\beta}{\alpha}\omega\left(1-\frac{3}{2}j_2\left[\frac{R}{a}\right]^2\left[4\cos^2 i-\frac{\beta}{\alpha}\cos i-1\right]\right)\ . \tag{7}$$

The ratio β/α in Eq. 7 depends on the orbital inclination and altitude. In this paper, an eccentricity $e = 0.001$ and an inclination of $i = 89.5°$ for both pendulum and GRACE configurations are selected, so one can focus here on the change of repeat sub-satellite tracks according to different orbital altitudes. Figure 1 shows different satellite orbits revolutions and their projected sub-satellite tracks on an Earth's map with the ratio β/α equal to 31/2, 170/11, 448/29, 247/16, and 108/7, corresponding to the orbital altitudes of 407, 410, 212, 415, and 420 km, respectively.

The selection of those orbital altitudes is based on the fact that the gravitational signal rapidly decays due to the so-called inverse attenuation factor, $[r/R_e]^{2n+1}$, which is a function of the spherical harmonic degree n. The term r

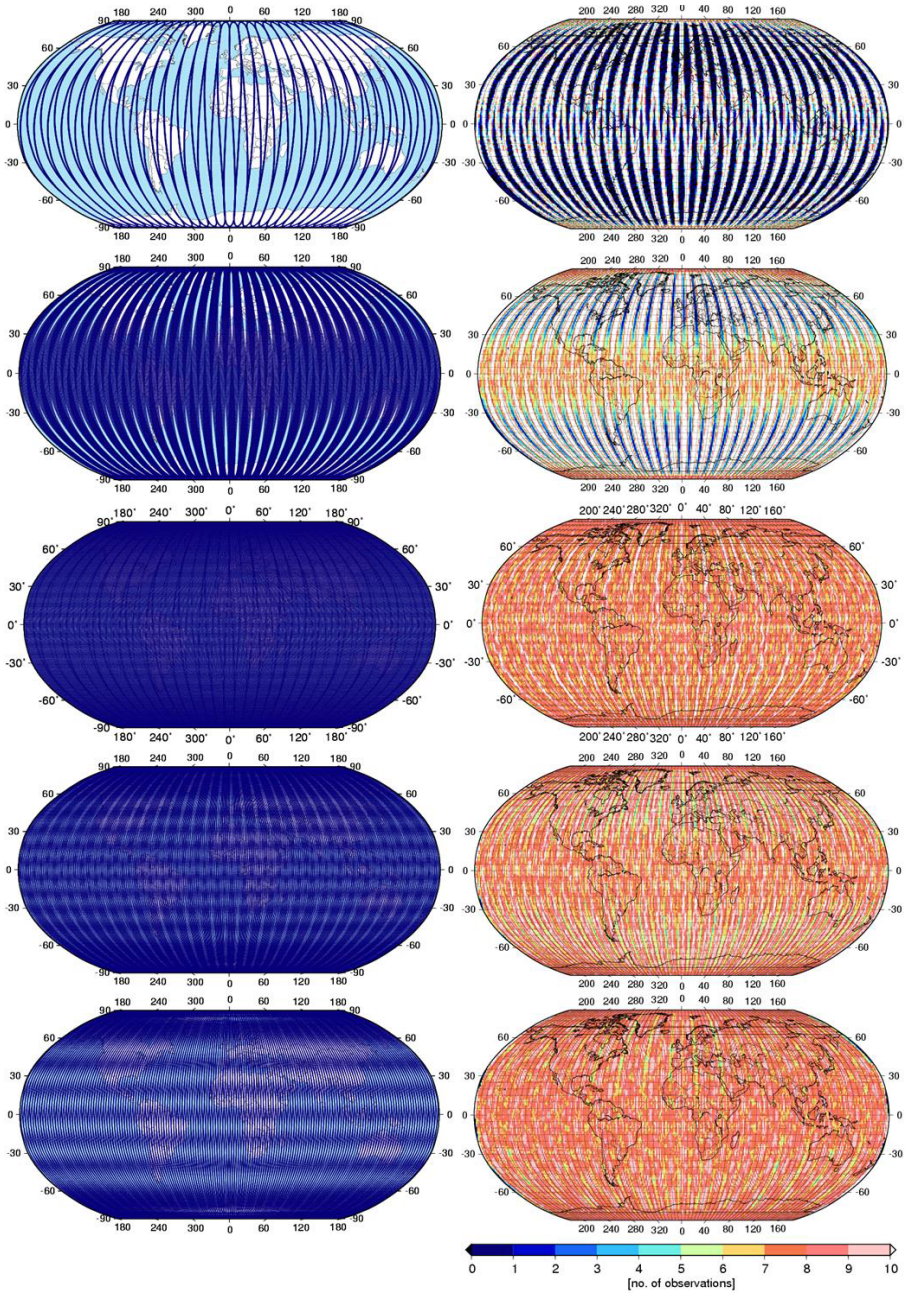

Fig. 1. Different satellite orbit revolutions (left column) and their corresponding projected sub-satellite tracks on the Earth's surface (right column) for different orbital altitudes; from top to bottom: repeat sub-satellite tracks with the ratios β/α of 31/2 (407 km), 170/11 (410 km), 448/29 (412 km), 247/16 (415 km), and 108/7 (420 km).

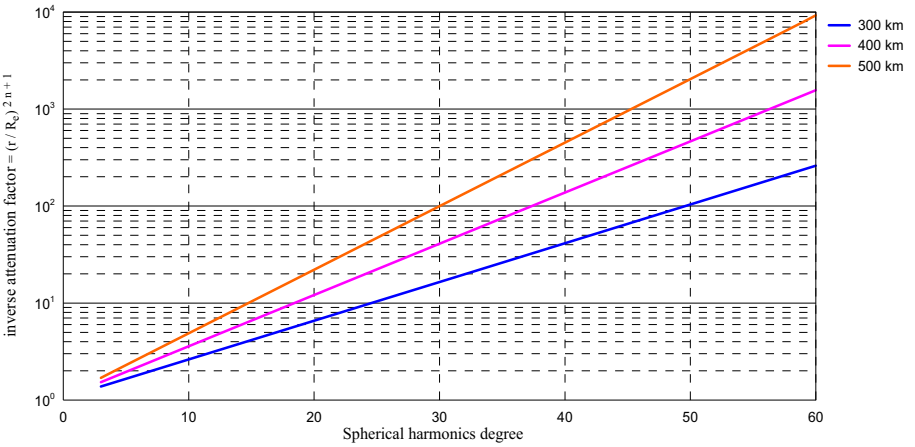

Fig. 2. The inverse attenuation factor showing the effect of orbital altitude on the gravity field recovery.

stands for the orbit altitude and R_e stands for the Earth's radius. The exponent n indicates that the higher the orbital altitude (and consequently the larger the r), the worse the resolution of the gravity field recovery (see, *e.g.*, Fig. 2).

Therefore, nearby orbital altitudes between 407 and 420 km are selected here in order to achieve different repeat modes without affecting the strength of the gravitational signal. The selected orbital altitudes represent different sub-satellite tracks that cover the Earth, insufficiently and sufficiently, as shown in Fig. 1.

3. PENDULUM AND GRACE MISSION CONFIGURATIONS

The GRACE-type configuration (Fig. 3, left panel) is considered as a simple collinear formation flying with two identical satellites separated from each other by approximately 220 km. The GRACE observables are sensitive only in an along-track direction. This is considered as the main drawback of the configuration geometry that no measurement information of the gravitational signal is collected in the cross-track and the radial direction. Therefore, one sees clearly a distortion of the monthly GRACE gravity estimates in the form of a longitudinal striping pattern. A common measure to counteract these effects is filtering the solutions (see, *e.g.*, Swenson and Wahr 2006, Kusche 2007); however, it is known that these procedures remove not only errors but signals as well.

It is generally accepted that follow-on missions should improve in sensitivity and isotropy by involving cross-track or radial information in the satellite observables. Radial information can be gathered via cartwheel and LISA

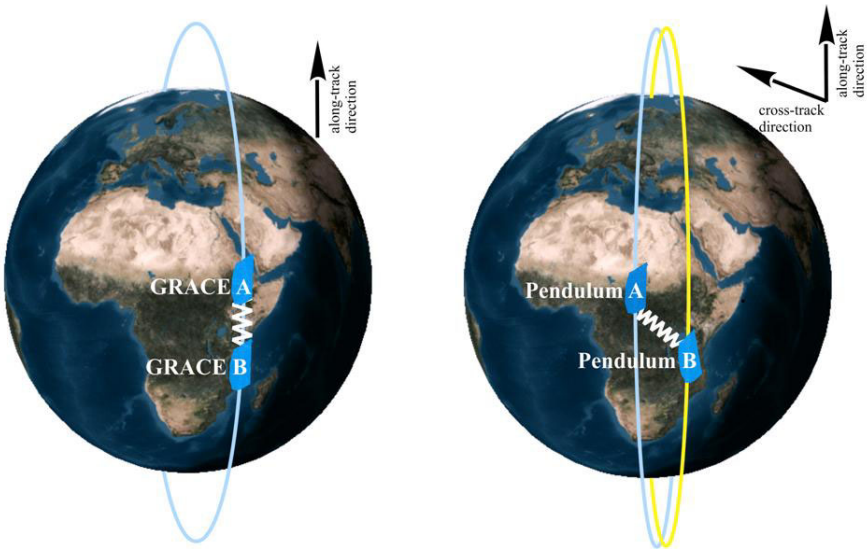

Fig. 3. The investigated satellite mission configurations: GRACE (left panel) and pendulum (right panel).

satellite mission scenarios, while cross-track information can be obtained via the pendulum mission scenario. Elsaka *et al.* (2012) has recommended the pendulum configuration as a future satellite-gravity mission candidate due to the relatively lower relative motion between its both satellites compared to the cartwheel and LISA configurations. Additionally, the pendulum mission was highly recommended by different scientific institutions as a future mission after GOCE (Gravity recovery and steady-state Ocean Circulation Explorer) era as proposed by the E.motion (Earth System Mass Transport Mission) team (see Panet *et al.* 2013) during the ESA (European Space Agency) call for proposals for Earth Explorer Opportunity Mission EE-8. However, they did not investigate the aliasing effects of ocean tides in their study. Therefore, the pendulum configuration at different sub-satellite track periods is considered here to investigate the aliasing errors of ocean tidal signal as a temporal gravity field. The cross-track link has been achieved between the two pendulum satellites by setting different angles of the right ascension of ascending nodes ($\Delta\Omega$) and of the mean anomaly ΔM (to achieve a non-zero cross-track component and to avoid the risk of collision of the two satellites). Another possibility to obtain cross-track formation with non-zero differential inclination is also achievable. However, this option is not guaranteed, since a non-trivial solution of the linear equation system exists (Sneeuw *et al.* 2008). Table 1 indicates the orbital parameters applied for both the GRACE and pendulum satellites. For comparative purposes, the

Table 1

Differential Keplerian orbital parameters
for the pendulum and GRACE missions

Orbital parameters	Formation flights	
	GRACE	Pendulum
Δa	0	0
Δe	0	0
Δi [deg]	0	0
$\Delta\Omega$ [deg]	0	0.45
$\Delta\omega$ [deg]	0	0
ΔM [deg]	1.72	1.72

inter-satellite distance of the pendulum configuration has been set similar to that of GRACE, *i.e.*, approximately 200 km (Fig. 4). At majority of the time, *i.e.*, from pole to equator or *vice versa*, the inter-satellite distance of the pendulum configuration contains a varying cross-track component (see Fig. 3, right panel). Yet, the pendulum configuration investigated here still fulfills requirements suggested by Elsaka *et al.* (2012), where the separation angle between the two satellites is 0.45° and with inter-satellite velocities of approximately ±8 m/s.

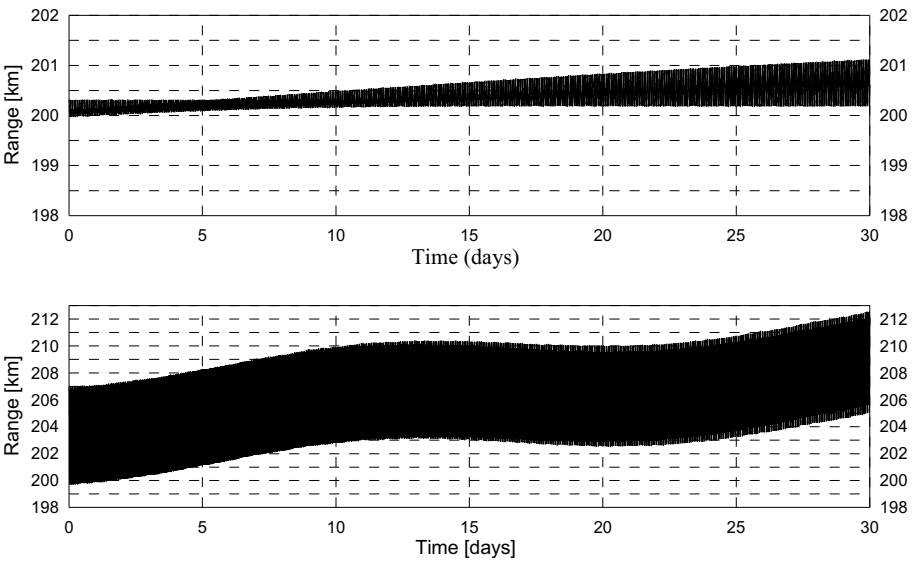

Fig. 4. The inter-satellite range (in km) for the investigated satellite configurations: GRACE (top panel) and pendulum (bottom panel).

4. SIMULATION STRATEGY

In order to compare the performance of both GRACE and pendulum configuration scenarios, numerical simulations using the Gravity Recovery Object Oriented Programming System (GROOPS) software have been performed. GROOPS has been developed in the Astronomical, Physical, and Mathematical Geodesy group at Bonn University to estimate gravity field parameters from satellite measurements, and it is routinely used to compute, *e.g.*, the ITG-GRACE solutions (see, *e.g.*, Mayer-Gürr *et al.* 2010). The mathematical description of GROOPS is given in details in Mayer-Gürr (2006).

For this study, all satellite orbits were integrated at 10-second steps using ITG-GRACE03s (Mayer-Gürr *et al.* 2010) as background mean gravity field model. In addition, background time-variable gravity field models have been used for ocean tidal forces as well as "non-tidal" atmospheric, "non-tidal" oceanic and hydrologic mass variations, as shown in Table 2. In the gravity analysis step, the same set of force models has been used except for the ocean tidal models to simulate the aliasing errors in the ocean tidal masses, as described in Section 1. Subsequently, each satellite orbit was corrupted with a Gaussian standard deviation of 1 cm to mimic errors of POD (precise orbit determination). The range measurements were nominally contaminated by white noise with standard deviation 50×10^{-9} m assuming the next generation of gravity missions will be equipped with a laser interferometric ranging system (Bender *et al.* 2003) as it is currently being developed for the GRACE follow-on mission. And therefore, this paper has not used accelerometer data for the pendulum scenario, as it has been set-up in this paper to be a drag-free mission. Moreover, applying higher noise levels (*e.g.*, micro levels in SST K-Band) leads to larger gravity field recovery errors than

Table 2

Background models applied to mean and time-variable simulation scenarios

Simulation scenario / Force function model	Measurement noise case		Oceanic tidal aliasing case	
	Orbit integration step	Gravity analysis step	Orbit integration step	Gravity analysis step
Mean field	ITG-GRACE03s	ITG-GRACE03s	ITG-GRACE03s	ITG-GRACE03s
Atmosphere	ECMWF	ECMWF	ECMWF	ECMWF
Ocean	OMCT	OMCT	OMCT	OMCT
Hydrology	WGHM	WGHM	WGHM	WGHM
Ocean tide	**FES2004**	**FES2004**	**FES2004**	**EOT08a**

the simulated tide model differences (*e.g.*, ocean tides) (see Visser *et al.* 2010, Elsaka 2010, p. 108).

Since this paper is focused mainly on the mitigation of aliasing errors induced in the oceanic tidal signal, we have decided to separate the impact of the error sources from the other time-varying non-tidal signals. This would help us to interpret the results more accurately regarding the effect of the shorter orbital repeating modes for minimizing the errors. Therefore, all models applied in the orbit integration step were reduced in the gravity analysis step. However, the investigated scenarios contain in reality some remaining aliasing errors that are resulting from the non-tidal signals, since we apply 6-hourly atmosphere and ocean models and daily hydrological model during the orbit integration step.

5. RESULTS

The results are provided in the "long-to-medium" spectral domain in terms of spherical harmonic coefficients up to degree/order (d/o) 60/60. The gravity field estimates are further visualized in terms of error degree-variances of the geoid heights, as shown in Figs. 5 and 6 for the measurement noise and oceanic tidal aliasing scenarios, respectively. In the spatial domain, geoid error maps are constructed in Fig. 7 for the oceanic tidal aliasing case. Moreover, Fig. 8 shows the gravity field solutions of the aliasing case considering only the individual semi-diurnal M2 tidal constituent determined by the pendulum configuration. The corresponding statistics in terms of global root mean square (RMS) values are given separately in Table 3. All error curves shown in Figs. 5 and 6 are obtained from the difference between outputs (estimates) and input (true model, *i.e.*, ITG-GRACE03s). This means that the mean field based on ITG-GRACE03s had to be removed from the monthly recovered solution in order to obtain the residual monthly gravity signal, due to the simulated error of the ocean tides signal.

As expected, all estimated solutions for the pendulum mission scenario perform approximately a half to one full order of magnitude (Table 3) better than the GRACE reference solution, in particular, at the medium wavelength range, as seen in Fig. 5 for the measurement noise case. However, Table 3 shows that the GRACE solutions at orbital heights of 410, 415, and 420 surpass those determined by the pendulum scenario. The reason is clearly identified in Fig. 5 that the pendulum configuration recover the harmonic coefficients at the long wavelength range (up to d/o 8) worse than the GRACE configuration. Yet the pendulum surpasses GRACE within the remaining long as well as medium range (*i.e.*, from d/o 9 up to d/o 60). According to the oceanic tidal aliasing case (Fig. 6), the pendulum solutions outperform the GRACE ones. This can be clearly seen in Table 3 and spatially on the

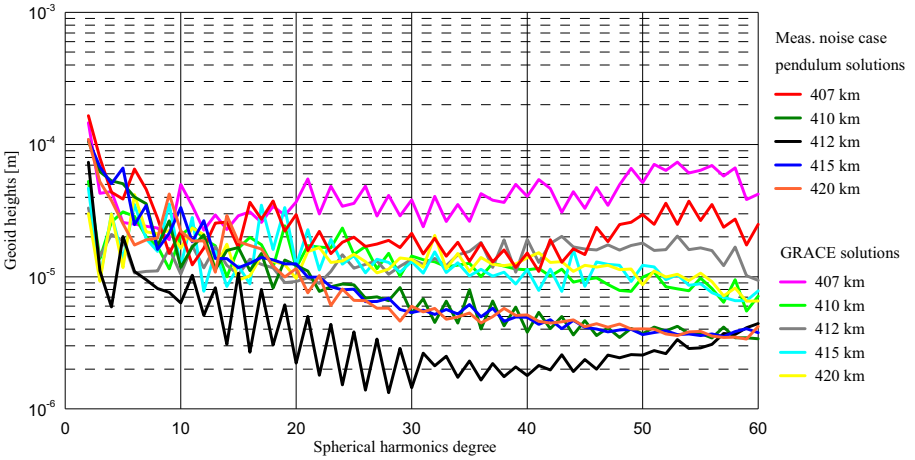

Fig. 5. Gravity solutions from the GRACE and pendulum mission scenarios in terms of error degree-variances of geoid heights for the measurement noise case.

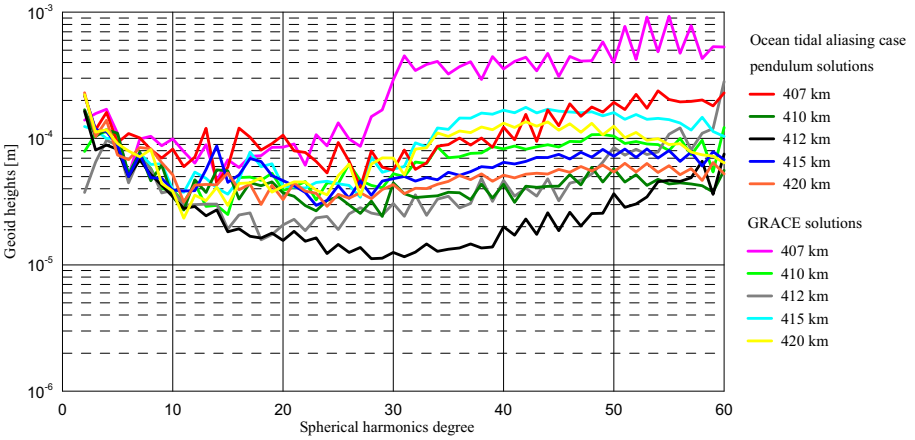

Fig. 6. Gravity solutions from the GRACE and pendulum mission scenarios in terms of error degree-variances of geoid heights for the ocean tidal aliasing case.

Earth's map in Fig. 7, which shows the global geoid height errors. The reason for this performance is that the pendulum configuration adds measurement information in the cross-track directions, and hence it helps in improving the retrieval of the mean and temporal gravity signal.

The north-south striping pattern has been obviously reduced via the pendulum gravity estimates in comparison to the GRACE reference solutions, which display a stronger striping pattern, as expected (see Fig. 7). This means that the pendulum configuration would not only be able to reduce aliasing errors but also to resolve the temporal signal better.

Fig. 7. Geoid height differences (in m) between the simulated static gravity field ITG-GRACE03s and the recovered solutions of the oceanic tidal aliasing case for the GRACE (left column) and pendulum (right column) mission scenarios according to the orbital heights from top to bottom: 407, 410, 412, 415, and 420 km.

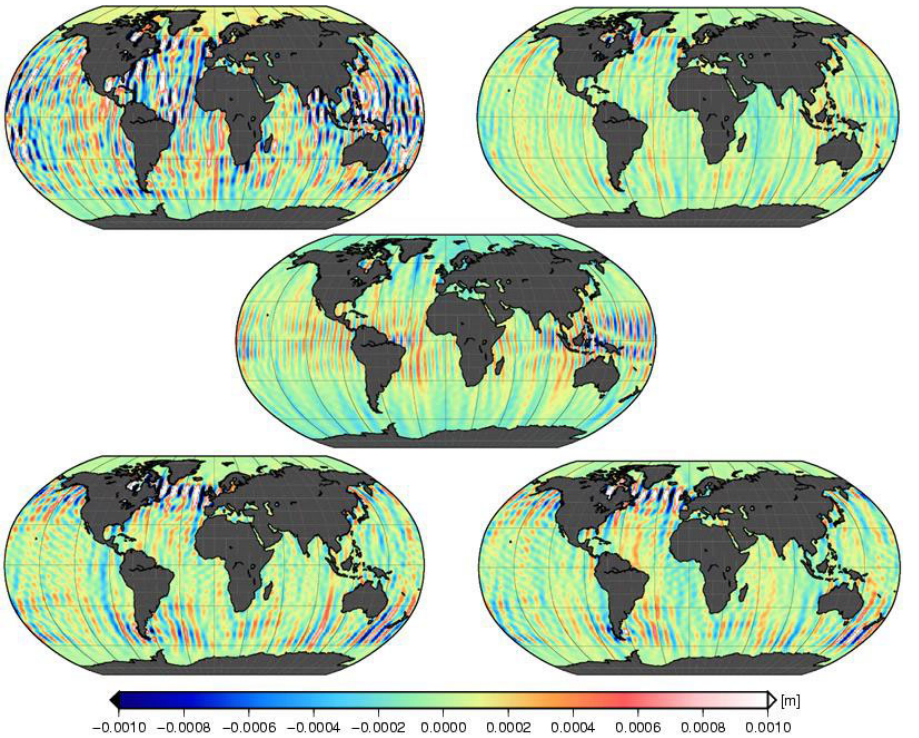

Fig. 8. Recovered solutions concerning the aliasing errors in M2 tidal constituent in terms of geoid height differences (in mm) for the pendulum mission scenarios according to the orbital heights of 407 km (top-left), 410 km (top-right), 412 km (middle), 415 km (bottom-left), and 420 km (bottom-right).

Table 3

Statistical values (RMS) in terms of geoid heights [mm] for both cases given in Table 2 determined by GRACE and pendulum configuration types at d/o 60 in addition to the M2 aliasing case

Orbital altitude [km]	Repeat period [days]	Measurement noise case (RMS)		Oceanic tidal aliasing case (RMS)		M2 aliasing case
		GRACE	Pendulum	GRACE	Pendulum	Pendulum
407	2	0.37	0.27	3.05	1.04	0.43
410	11	0.12	0.16	0.59	0.39	**0.16**
412	29	**0.11**	**0.07**	**0.51**	**0.32**	0.19
415	16	0.13	0.18	0.91	0.55	0.31
420	7	0.12	0.16	0.74	0.50	0.26

Note: bolded are the smallest RMS values.

According to the performance of the gravity field retrievals concerning the different repeating modes of sub-satellite tracks, one finds that the 29-day repeating mode provides the least oceanic tidal aliasing errors for both GRACE and pendulum configurations. This is due to the sufficient satellite observables and the adequate Earth coverage. Strong improvements have been found also for the 11-day repeating for mitigating the aliasing errors as seen in Table 3, which behaves similar to the 29-day repeating.

Since the pendulum configuration provides the least oceanic tidal aliasing errors, it has been additionally examined here how different repeating modes could mitigate the aliasing errors of the individual tides. For this case, the semi-diurnal M2 tidal constituent was selected. One can find here that both the 29-day and 11-day repeating still result in similar improvements; however, the 11-day repeating outperforms the 29-day repeating. This can be seen in Fig. 8 showing that the M2 aliasing errors have been minimized by the 11-day repeating mode better than by the other repeating modes.

One can infer that although the 29-day solution may be the best choice for minimizing the temporal aliasing errors, its temporal resolution is still not enough to resolve errors in the individual temporal signals. Therefore, it is recommended that the pendulum, as a candidate for a future gravity mission for detecting the temporal variations of the Earth's gravity field, is flown in a 29-day repeating mode allowing sufficient satellite observations with, *e.g.*, 11-day sub-cycle repeating at the same time to allowing a better understanding of the temporal variations of the individual time-varying signals.

6. CONCLUSION

In the course of this paper, the effect of different repeating modes concerning the sub-satellite tracks of the pendulum configuration has been investigated for the mitigation of the oceanic tidal aliasing errors.

The first conclusion is that the aliasing errors in the ocean tides reduce significantly if moderate cross-track components are added to the SST observable. This is in principle expected to be beneficial when the satellite pair flies in alternative configuration, such as the pendulum mission. One can also confirm the earlier findings that the GRACE formation is sub-optimal in terms of the gravity field retrievals. Second, it has been found that the selection of proper "shorter" repeating sub-satellite tracks provides a better understanding of the aliasing errors than the longer repeating mode. The 29-day repeating mode ensures a sufficient global Earth coverage; however, it has been found that it cannot resolve the temporal aliasing effects of the individual ocean tides constituents (*e.g.*, M2 semi-diurnal signal). On the other hand, the 11-day repeating mode could resolve the ocean tidal aliasing errors of individual constituents better.

Finally, it is recommended that a future gravity mission is launched in an orbital altitude of 29-day repeating cycle implementing at the same time 11-day repeating sub-cycle, which would support the detection of mass variations at higher temporal frequencies.

Acknowledgements. The authors would like firstly to thank the Managing Editor, Dr. Z. Wisniewski, for his efforts during the publication process of this manuscript and would like also to thank the reviewers for their valuable comment. The financial support of King Abdulaziz City for Science and Technology (KACST) is gratefully acknowledged.

References

Bender, P.L., J.L. Hall, J. Ye, and W.M. Klipstein (2003), Satellite-satellite laser links for future gravity missions, *Space Sci. Rev.* **108**, 1-2, 377-384, DOI: 10.1023/A:1026195913558.

Bender, P.L., D.N. Wiese, and R.S. Nerem (2008), A possible dual-GRACE mission with 90 degree and 63 degree inclination orbits. **In:** *Proc. Third Int. Symp. on Formation Flying, Missions and Technologies, 23-25 April 2008, Noordwijk, Netherlands*, 23-25.

Bezděk, A., J. Klokočnik, J. Kostelecky, R. Floberghagen, and C. Gruber (2009), Simulation of free fall and resonances in the GOCE mission, *J. Geodyn.* **48**, 1, 47-53, DOI: 10.1016/j.jog.2009.01.007.

Elsaka, B. (2010), Simulated satellite formation flights for detecting the temporal variations of the Earth's gravity field, Ph.D. Thesis, University of Bonn, Bonn, Germany.

Elsaka, B. (2014), Sub-monthly gravity field recovery from simulated multi-GRACE mission type, *Acta Geophys*. **62**, 1, 241-258, DOI: 10.2478/s11600-013-0170-9.

Elsaka, B., J. Kusche, and K.-H. Ilk (2012), Recovery of the Earth's gravity field from formation-flying satellites: Temporal aliasing issues, *Adv. Space Res.* **50**, 11, 1534-1552, DOI: 10.1016/j.asr.2012.07.016.

Elsaka, B., J.-C. Raimondo, P. Brieden, T. Reubelt, J. Kusche, F. Flechtner, S. Iran Pour, N. Sneeuw, and J. Müller (2014a), Comparing seven candidate mission configurations for temporal gravity field retrieval through full-scale numerical simulation, *J. Geod.* **88**, 1, 31-43, DOI: 10.1007/s00190-013-0665-9.

Elsaka, B., E. Forootan, and A. Alothman (2014b), Improving the recovery of monthly regional water storage using one year simulated observations of two pairs of GRACE-type satellite gravimetry constellation, *J. Appl. Geophys.* **109**, 195-209, DOI: 10.1016/j.jappgeo.2014.07.026.

Förste, C., R. Schmidt, R. Stubenvoll, F. Flechtner, U. Meyer, R. König, H. Neumayer, R. Biancale, J.-M. Lemoine, S. Bruinsma, S. Loyer, F. Barthelmes, and S. Esselborn (2008), The GeoForschungsZentrum Potsdam/Groupe de Recherche de Gèodésie Spatiale satellite-only and combined gravity field models: EIGEN-GL04S1 and EIGEN-GL04C, *J. Geod.* **82**, 6, 331-346, DOI: 10.1007/s00190-007-0183-8.

Kaula, W.M. (1966), *Theory of Satellite Geodesy*. *Applications of Satellites to Geodesy*, Blaisdell Publ. Co., Waltham.

Kusche, J. (2007), Approximate decorrelation and non-isotropic smoothing of time-variable GRACE-type gravity field models, *J. Geod.* **81**, 11, 733-749, DOI: 10.1007/s00190-007-0143-3.

Lyard, F., F. Lefevre, T. Letellier, and O. Francis (2006), Modelling the global ocean tides: modern insights from FES2004, *Ocean Dynam.* **56**, 5-6, 394-415, DOI: 10.1007/s10236-006-0086-x.

Mayer-Gürr, T. (2006), Gravitationsfeldbestimmung aus der Analyse kurzer Bahnbögen am Beispiel der Satellitenmissionen CHAMP und GRACE, Ph.D. Thesis, University of Bonn, Bonn, Germany.

Mayer-Gürr, T., A. Eicker, E. Kurtenbach, and K.-H. Ilk (2010), ITG-GRACE: Global static and temporal gravity field models from GRACE data. **In:** F.M. Flechtner, T. Gruber, A. Güntner, M. Mandea, M. Rothacher, T. Schöne, and J. Wickert (eds.), *System Earth via Geodetic-Geophysical Space Techniques*, Springer, Berlin Heidelberg, 159-168, DOI: 10.1007/978-3-642-10228-8_13.

Panet, I., J. Flury, R. Biancale, T. Gruber, J. Johannessen, M.R. van den Broeke, T. van Dam, P. Gegout, C.-W. Hughes, G. Ramillien, I. Sasgen, L. Seoane, and M. Thomas (2013), Earth system mass transport mission (e.motion): A concept for future earth gravity field measurements from space, *Surv. Geophys*. **34**, 2, 141-163, DOI: 10.1007/s10712-012-9209-8.

Rees, W.G. (2001), *Physical Principles of Remote Sensing*, 2nd ed., Cambridge University Press, Cambridge, 343 pp.

Savcenko, R., and W. Bosch (2008), EOT08a – empirical ocean tide model from multi-mission satellite altimetry, Rep. No. 81, Deutsches Geodätisches Forschungsinstitut (DGFI), München, Germany.

Sharifi, M., N. Sneeuw, and W. Keller (2007), Gravity recovery capability of four generic satellite formations. **In:** A. Kiliçoglu, and R. Forsberg (eds.), *Proc. Symp. "Gravity Field of the Earth", General Command of Mapping*, *June 2007, Ankara, Turkey*, Spec. Issue 18, 211-216.

Sneeuw, N., M.A. Sharifi, and W. Keller (2008), Gravity recovery from formation flight missions. **In:** P. Xu, J. Liu, and A. Dermanis (eds.), *VI Hotine-Marussi Symposium on Theoretical and Computational Geodesy*, International Association of Geodesy Symposia, Vol. 132, Springer, Berlin Heidelberg, 29-34, DOI: 10.1007/978-3-540-74584-6_5.

Swenson, S., and J. Wahr (2006), Post-processing removal of correlated errors in GRACE data, *Geophys. Res. Lett.* **33**, 8, L08, 402, DOI: 10.1029/2005GL025285.

Tapley, B.D., S. Bettadpur, M. Watkins, and C. Reigber (2004), The gravity recovery and climate experiment: Mission overview and early results, *Geophys. Res. Lett.* **31**, 9, DOI: 10.1029/2004GL019920.

Visser, P.N.A.M., N. Sneeuw, T. Reubelt, M. Losch, and T. van Dam (2010), Space-borne gravimetric satellite constellations and ocean tides: aliasing effects, *Geophys. J. Int.* **181**, 2, 789-805, DOI: 10.1111/j.1365-246X.2010.04557.x.

Wahr, J., S. Swenson, V. Zlotnicki, and I. Velicogna (2004), Time-variable gravity from GRACE: First results, *Geophys. Res. Lett.* **31**, 11, L11501, DOI: 10.1029/2004GL019779.

Wiese, D.N., W.M. Folkner, and R.S. Nerem (2009), Alternative mission architectures for a gravity recovery satellite mission, *J. Geod.* **83**, 6, 569-581, DOI: 10.1007/s00190-008-0274-1.

Wiese, D.N., R.S. Nerem, and S.-C. Han (2011a), Expected improvements in determining continental hydrology, ice mass variations, ocean bottom pressure signals, and earthquakes using two pairs of dedicated satellites for temporal gravity recovery, *J. Geophys. Res.* **116**, B11, B11405, DOI: 10.1029/2011JB008375.

Wiese, D.N., P. Visser, and R.S. Nerem (2011b), Estimating low resolution gravity fields at short time intervals to reduce temporal aliasing errors, *Adv. Space Res*. **48**, 6, 1094-1107, DOI: 10.1016/j.asr.2011.05.027.

Wiese, D.N., R.S. Nerem, and F.G. Lemoine (2012), Design considerations for a dedicated gravity recovery satellite mission consisting of two pairs of satellites, *J. Geod.* **86**, 2, 81-98, DOI: 10.1007/s00190-011-0493-8.

Received 30 October 2013
Received in revised form 19 August 2014
Accepted 3 September 2014